Journal of Sol-Gel Science and Technology
https://doi.org/10.1007/s10971-025-06763-z

ORIGINAL PAPER

Elaboration and characterization of ZnO/CuO nano-composites produced by sol-gel route for supercapacitor application

Mohd Oulmessaoud Boughanem[1,2] · Nassim Touka[1,2] · Salim Mokhtari[3] · Salima Kaizra[4,5] · Salah Eddine Berrabah[4] · Dalila Tabli[1,2] · Nourddine Selmi[6] · Mohamed Trari[7]

Received: 14 February 2025 / Accepted: 10 April 2025

Abstract

In the present work, CuO with concentration of 0.15 mol/L, ZnO with a concentration of 0.25 mol/L, and ZnO/CuO Nano composites with following ratios (50% ZnO & 50% CuO and 70% ZnO & 30% CuO) were prepared and deposited on glass substrates by the sol-gel spin coating process. Physical techniques such as X-ray diffraction analysis (XRD), atomic force microscopy, and UV-Vis spectroscopy were used for the characterization of the crystal structure, surface topography, and optical properties. The XRD analysis showed that CuO and ZnO crystallize respectively in monoclinic and hexagonal symmetries. Crystallite size decreased while dislocation density and microstress increased upon addition of CuO. These increases are responsible for the reduction in crystallite size. The AFM microscopy demonstrates alteration in the surface morphology, with inclusion of CuO leading to decrease in the average roughness (Ra) of ZnO. The UV-Vis spectrophotometry indicate that the band edge absorption is red-shifted whereas 50%ZnO/50%CuO is highly red-shift in spectra. The gap energies (Eg) of 1.73, 3.25, 3.19, and 2.88 eV are found respectively for CuO, ZnO, 70%ZnO/30%CuO and 50%ZnO/50%CuO. The films exhibit high super-capacitor properties, the electrochemical study showed that the electrode 50% ZnO/50%CuO has high specific capacitance of 217.81 F/g at 1 mV/s and excellent cyclic stability with nearly 96% capacity retention after 5000 cycles at 0.1 mA/cm^2.

Graphical Abstract

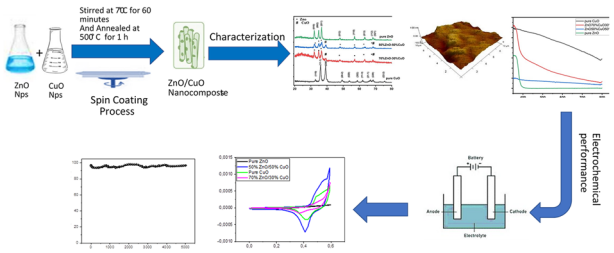

Keywords Sol-gel · Spin coating · ZnO/CuO Nano-composite · Energy gap

✉ Salim Mokhtari
s.mokhtari@univ-bouira.dz

1 Materials and Sustainable Development Laboratory, University of Bouira, Bouira, Algeria

2 Physics of Materials and Optoelectronic Components Laboratory. Department of Physics, Faculty of Sciences and Applied Sciences, University of Bouira, Bouïra, Algeria

3 Processes for Materials, Energy, Water and Environment, University of Bouira, Bouira, Algeria

4 Laboratory of Electrochemistry-Corrosion, Metallurgy and Inorganic Chemistry, Faculty of Chemistry (USTHB), 16111 Algiers, Algeria

5 Laboratory of N-body & Structure of Matter, Department of Physical Sciences, ENS-Kouba, Kouba, BP 92, Algiers 16308, Algeria

6 Nuclear Research Center of Birine, Djelfa, Algeria

7 Laboratory of Storage and Valorization of Renewable Energies, Faculty of Chemistry (USTHB), BP 32, Algiers 16111, Algeria

Published online: 28 April 2025

Highlights

- ZnO, CuO, and ZnO/CuO Nano-composites were successfully synthesized by sol-gel method.
- The influence of different composition ratios of ZnO/CuO Nano-composite on crystallite size.
- Investigation of the structural, morphological, and optical properties of ZnO/CuO Nano-composites.
- High super-capacitor and excellent cyclic stability of the 50%ZnO/50%CuO electrode.

1 Introduction

Nowadays, the production of Nano-materials has increased with numerous researches due to their unique properties and distinct characteristics. Among these Nano-materials, Nano-composites of ZnO and CuO have attracted great interest due to their potential applications in fields of solar cells [1], photocatalysis [2], lithium-ion batteries [3], sensors [4] and electronic [5].

Previous studies have investigated the synthesis and electrochemical performance of ZnO/CuO Nano-composites for super-capacitor applications. These studies have demonstrated that the morphology, composition, and synthesis method of the Nano-composites significantly influence their photocatalytic and electrochemical properties. For example, Wu and Wang [6], reported the synthesis of CuO/ZnO Nano-composite by solide-state reaction and achieved a specific capacitance of 579.5 F/g with 83% capacity retention after 2000 cycles at current density of 5 A/g. Similarly, Bishwakarma and Kumar [7] prepared CuO/ZnO Nano-composite using one-step electrochemical discharge process and obtained a specific capacitance of 313 F/g at 2 A/g current density and 84.1% retention capacitance after 5000 cycles. Despite the progress made in the development of ZnO/CuO Nano-composites for super-capacitors, several research gaps remain. These include the need to improve cycling stability. Although ZnO/CuO Nano-composites exhibit good initial capacity, their cycling stability often deteriorates over time. Current research aims to address these gaps by developing strategies to improve the cycling stability of Nano-composites through surface modification, electrolyte optimization, and device design. By addressing these gaps, this study aims to contribute to the development of high-performance ZnO/CuO Nano-composites for super-capacitor applications.

ZnO is a wide band gap semiconductor with ***n***-type conduction, due to oxygen vacancies. It crystallizes a hexagonal Wurtzite structure and a band gap of ~3.2 eV, depending on the synthesis method, a high exciton binding energy (60 meV), and transparency over the visible region [8]. Because of its low cost, structural and chemical stabilities and sensitivity to UV-light, it is regarded as a favorable material for photocatalytic and photo-electrochemical applications [9]. On the other side, CuO is a narrow band semiconductor material with ***p***-type conductivity. It crystallizes in a monoclinic structure and possesses an ideal band gap (~1.4 eV), chemical stability [10] and is commonly used in sensing applications and photocatalysis [11].

Nano-composite materials can be synthesized by different methods, including coprecipitation [12], spray pyrolysis [13], sol-gel method [14], and pulsed laser deposition [15]. These techniques provide the ability to control the size, shape, and composition of the metal oxide, which subsequently influence their semiconductor properties and photocatalytic performance. Among these techniques, the sol-gel method is attractive since it produces enhanced active surface areas with a narrow size distribution. It has various advantages, namely cost-effective and control of chemical homogeneity with easily achievable approach.

This work focuses on the deposition of CuO and ZnO, as well as Nano-composites (50% ZnO/50% CuO) and (70% ZnO/30% ZnO) on glass substrates by sol-gel spin-coating technique. The main objective was to study the impact on physical, morphological and optical properties. For electrochemical characterization, cyclic voltammetry was used to evaluate the capacitive behavior, specific capacitance and scan rate effects. Galvanostatic charge-discharge experiments provided insights into stability, highlighting the suitability of these materials for energy storage applications.

2 Experimental

2.1 Synthesis of ZnO/CuO nanocomposites

First, the glass substrates underwent a cleaning procedure with hydrochloric acid (HCl) and acetone, followed by rinsing with distilled water and sonication using an ultrasonic cleaner. Then, pure ZnO Nano-particles were prepared by dissolving 1.376 g zinc acetate anhydrous.

The glass substrates were first cleaned with HCl and acetone, rinsed with distilled water, and sonicated using an ultrasonic cleaner. ZnO Nan-oparticles were prepared by dissolving 1.376 g of Zn $(CH_3COO)_2$ (98% sigma Aldrich) in 30 mL of ethanol with 0.458 g of mono-ethanolamine (MEA) (99% Biochem) to obtain a concentration of 0.25 mol/L. The solution was stirred at 70 °C for 1 h under magnetic agitation [16, 17]. The synthesis of CuO Nano-particles involved dissolving 0.89 g of copper acetate monohydrate $Cu(CO_2CH_3)_2.H_2O$ (98% Sigma Aldrich) in 30 mL of propanol (IPA) together with 0.3 mL of MEA to achieve a concentration of 0.15 mol/L. The solution was

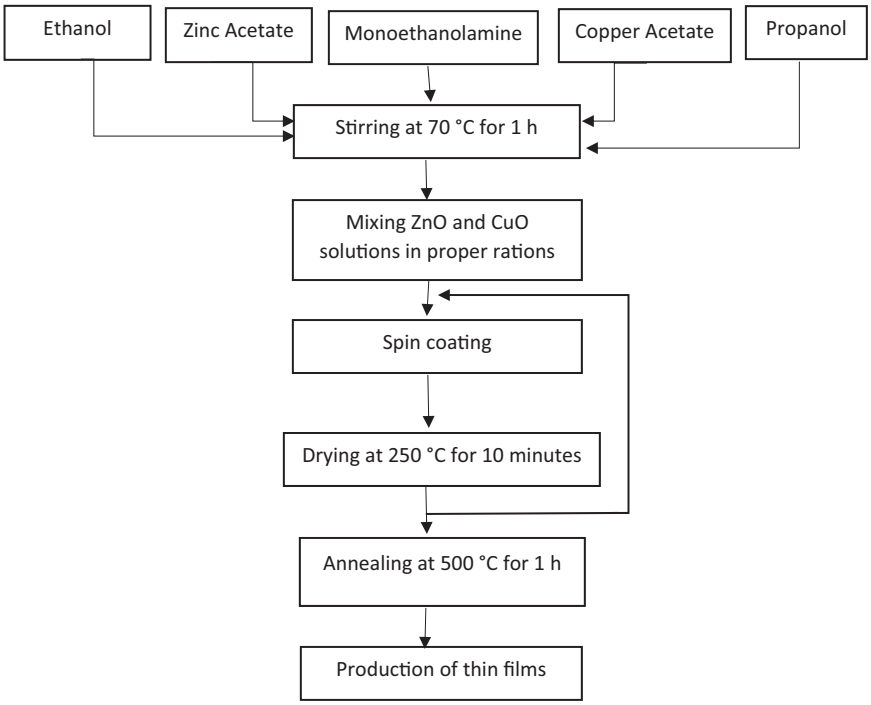

Fig. 1 Flow diagram of the ZnO, CuO and ZnO/CuO Nano-composites thin film production process

stirred at 70 °C for 1 h [15]. Both solutions were subjected to sonication for 10 min at 50 °C.

Two ratios of the ZnO/CuO Nano-composites were prepared by mixing 70% ZnO solution with 30% CuO solution and 50% ZnO with 50% CuO. The mixed solutions were stirred at 70 °C for 1 h and then filtered using filter paper to remove undissolved particles [18].

Finally, deposition of all solutions was carried out on glass substrates by centrifugation at 2800 rpm for 60 s, followed by drying at 250 °C for 10 min. on a hot plate. This procedure was repeated twice to obtain two layers. All samples were annealed for 1 h in open air at 500 °C.

The instrument XPERT-PRO MPD of Panalytical with Cu radiation ($\lambda = 1.5406$ Å), 30.0 kV, and 40.0 mA was employed to study the structure and microstructure of thin films produced.

The optical properties were studied by using the UV-Vis spectrophotometer Jasco V-750 in the range (50–800 nm), PTFE was used as reference.

2.2 Electrode preparation

The electrochemical experiments were carried out in a sealed container using a three-electrode system. Pt gauze was used as a counter-electrode, while a saturated calomel electrode (SCE) served as a reference [19]. The working electrodes were fabricated from the following samples: ZnO, CuO, a mixture of 70% ZnO and 30% CuO, and a mixture of 50% ZnO and 50% CuO; KOH (1 M) was used as electrolyte. A Solartron electrochemical workstation (model SI 1287-1260) managed by CorrView software was employed for the electrochemical tests.

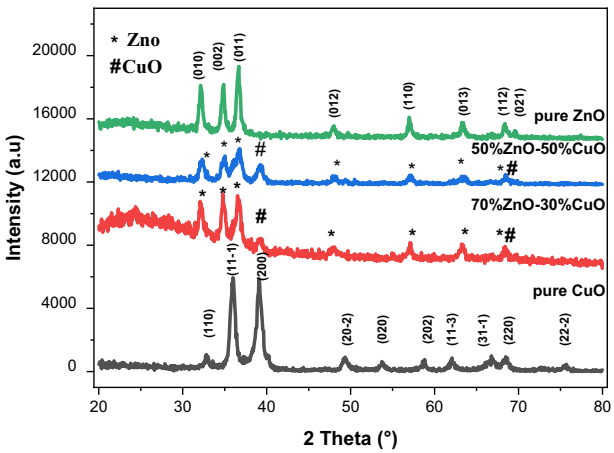

Fig. 2 XRD patterns of ZnO, CuO, 50%ZnO/50%CuO, and 70%ZnO/30%CuO thin films

3 Results and discussions

3.1 XRD analysis

Figure 1 shows the experimental protocol for ZnO/CuO deposited on glass substrates by the sol-gel spin coating process Fig. 2 shows the crystal planes for ZnO are (010), (002), (011), (012), (110), (013), (112), and (021) observing

Table 1 Structural parameters of CuO/ZnO thin films

Sample	Size D (nm)	Dislocation density δ *(10)^{15}	Microstrain ε* (10^{-3})
CuO	12.88	6.02	8.8
ZnO	18.06	3.06	6.4
70%ZnO/ 30%CuO	15.24	4.3	7.7
50%ZnO/ 50%CuO	11.73	7.26	10

at 2θ = 32.16, 34.81, 36.63, 47.95, 57.01, 63.36, 68.38 and 69.61°, respectively, are in accordance with hexagonal wurtzite ZnO structure (JCPDS card N°: 98-015-4487) [20].

The XRD peaks of CuO are observed at 2θ = 32.86, 35.97, 39.11, 49.34, 53.76, 58.73, 62.07, 66.71, 68.45 and 75.56°, which correspond to the (110), (11-1), (200), (20-2), (020), (202), (11-3), (31-1), (220) and (22-2) planes, in that order. Are assigned to be monoclinic CuO structure (JCPDS card number: 98-065–3723) [21].

The XRD peaks for ZnO/CuO nanocomposites with different ratios are (010), (002), (011), (012), (110), (013), and (112) planes according to jcpds data of ZnO and (200), (220) planes according to JCPDS data of CuO. The prepared samples show single phases with a high purity, as only ZnO and CuO are composed; not observed other phases, such as Cu_2O. The sizes of crystallites (D), dislocation density (δ), and microstrain (ε) were calculated from the following relations [22, 23] and given in Table 1.

$$D = \frac{0.9 * \lambda}{\beta \cos \theta} \quad (1)$$

$$\delta = 1/D^2 \quad (2)$$

$$\epsilon = \beta/4 \tan \theta \quad (3)$$

where β the measurement of the full width at half maximum of the peak, and θ the diffraction peak.

The results (Table 1) indicate a decrease of the crystallite size with increasing the CuO concentration due to the influence of defects caused by Cu^{2+} within the ZnO lattice structure [24, 25], due to the slight difference in ionic radii between Zn^{2+} (0.60 Å) and Cu^{2+} (0.62 Å) [22]. The increase of the dislocation density is associated with the increase of the microstrain within the Nano-composites, which contributes to the reduction in the crystallite size, as the internal stresses can prevent the formation of larger crystal domains [22, 26].

3.2 Surface morphological analysis

The morphological properties were examined using (MFP-3D-SA) (AFM) (area of 10 μm by 10 μm) (Fig. 3).

The average surface roughness (Ra) and the root mean square (Sq), measured by Gwydion software, are given in Table 2.

According to the literature [27, 28], addition of CuO has modified the morphology of ZnO layers and reduced the roughness (Ra) due to incorporating particles within the Nano-composites. It is also noted that the roughness of ZnO/CuO decreases with decreasing the CuO content.

3.3 Optical properties analysis

UV-Vis absorbance was measured in the spectral range (50–800 nm). Figure 4 shows that pure ZnO has a high absorbance in the UV region and is transparent over the visible region. On the other hand, CuO has broad-range absorption in the UV-Visible region. The addition in CuO concentration improved the absorbance intensity of ZnO, and simultaneously the band edge absorption is red-shifted [29, 30].

The gap energy (E_g) of all samples are determined to use the well-known relationship [28]:

$$(\alpha h\nu)^n = \text{Const}(h\nu - Eg) \quad (4)$$

where α is the coefficient of absorption (α = 2.303 A/d) whose inverse is equal to the penetration length of monochromatic radiation (λ), ***A*** the absorbance, ***d*** the thickness obtained by using PLASMOS SD 2000 ellipsometer for 06 different points of each sample) and ***hν*** the photon energy (eV), the exponent ***n*** indicates the nature of the transition. The gap E_g of all samples are determined by extrapolating the linear part of $(\alpha h\nu)^2$ to the x-axis, as depicted in Fig. 5 and Table 3. It is important to note that the bandgap values reported here are based on the Tauc approximation, which assumes a homogeneous and continuous thin film structure.

The inclusion of CuO shifts the gap of Nano-composites toward lower energies. The phenomenon is due to an enhanced combined transition involving (O^{2-}: ***2p***) → Zn^{2+}: ***3d^{10}-4s***) and (O^{2-}: ***2p***) → Cu^{2+}: ***3d^9***) [25, 31].

3.4 Electrochemical performance

Figure 6 presents the cyclic voltammograms of the different samples, recorded at various scan rates. Oxidation and reduction peaks were observed at ~0.4 V and 0.55 V *vs.* SCE, respectively, indicating a quasi-reversible behavior of the electrode materials [32]. A slight shift toward more anodic and cathodic potentials occurs with increasing the scan rate [32, 33]. The comparison highlights the electrochemical behavior of each film at different sweeping rates, thus providing information on their capacitive properties and charge storage mechanisms.

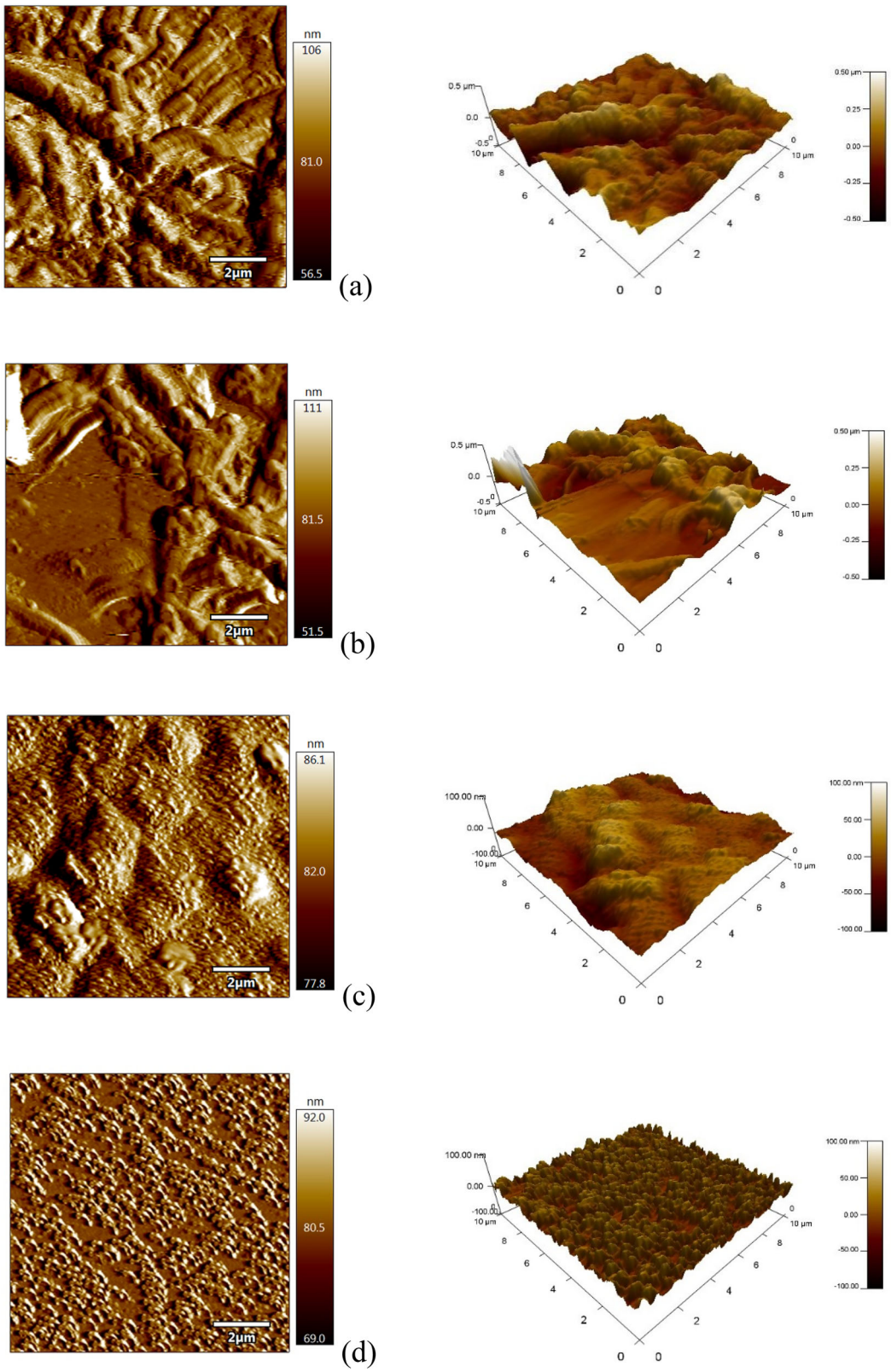

Fig. 3 3D and 2D atomic force microscope (AFM) images of pure ZnO (**a**), pure CuO (**b**), 50%ZnO/50%CuO (**c**), and 70%ZnO/30%CuO (**d**)

Table 2 Surface roughness parameters of all samples

samples	RMS (Sq) (nm)	(Ra) (nm)
CuO	101.126	73.607
ZnO	85.337	65.668
70%ZnO/30%CuO	12.553	10.703
50%ZnO/50%CuO	15.742	12.537

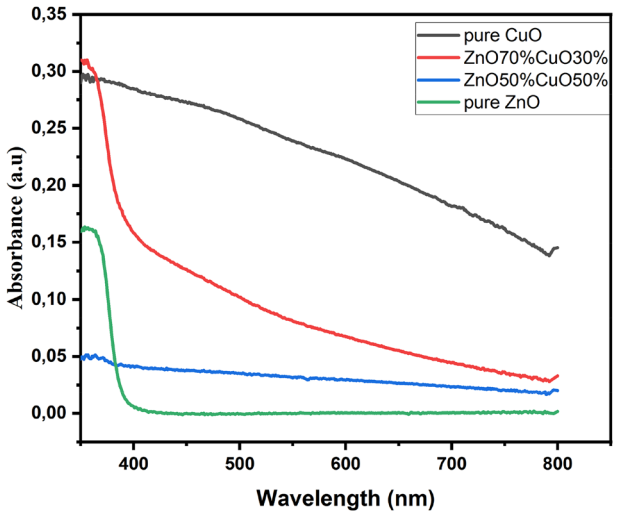

Fig. 4 UV-vis absorption spectra of samples pure ZnO, pure CuO, 50%ZnO/50%CuO, and 70%ZnO/30%CuO

All samples exhibit battery-type supercapacitor behavior, characterized by distinct oxidation and reduction peaks in their cyclic voltammograms in the region (0.0–0.6 V_{SCE}). Moreover, the curves maintain stable shapes even at high speeds, indicating good flow capacity of the processed oxides.

Figure 7 shows the CV curves at a scan rate of 10 mV/s, where 50%ZnO – 50%CuO sample demonstrates the highest oxidation and reduction peaks. This enhancement is attributed to the improved redox activity and synergistic effects between ZnO and CuO, where faradaic processes in charge storage is involved [34]. To calculate the specific capacitance from the cyclic voltammograms, we used the following formula [9]:

$$Cs = \frac{\int \mathrm{I(V)dV}}{\mathrm{m}.\Delta \mathrm{V}.\mathrm{v}} \tag{5}$$

Where:

Table 3 Optical gap of CuO, ZnO and ZnO/CuO Nano-composites

Oxide	Thickness (nm)	E_g (eV)
CuO	194	1.73
ZnO	202	3.25
70%ZnO/30%CuO	151	3.19
50%ZnO/50%CuO	187	2.88

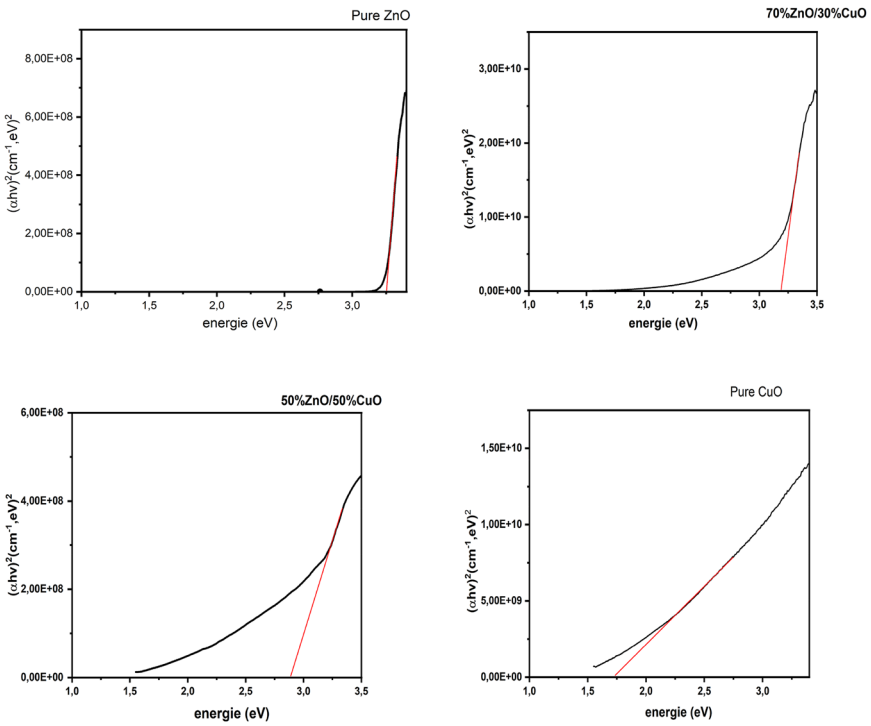

Fig. 5 Determination of the optical gap (E_g) of ZnO, CuO, 50%ZnO/50%CuO, and 70% ZnO/30%CuO

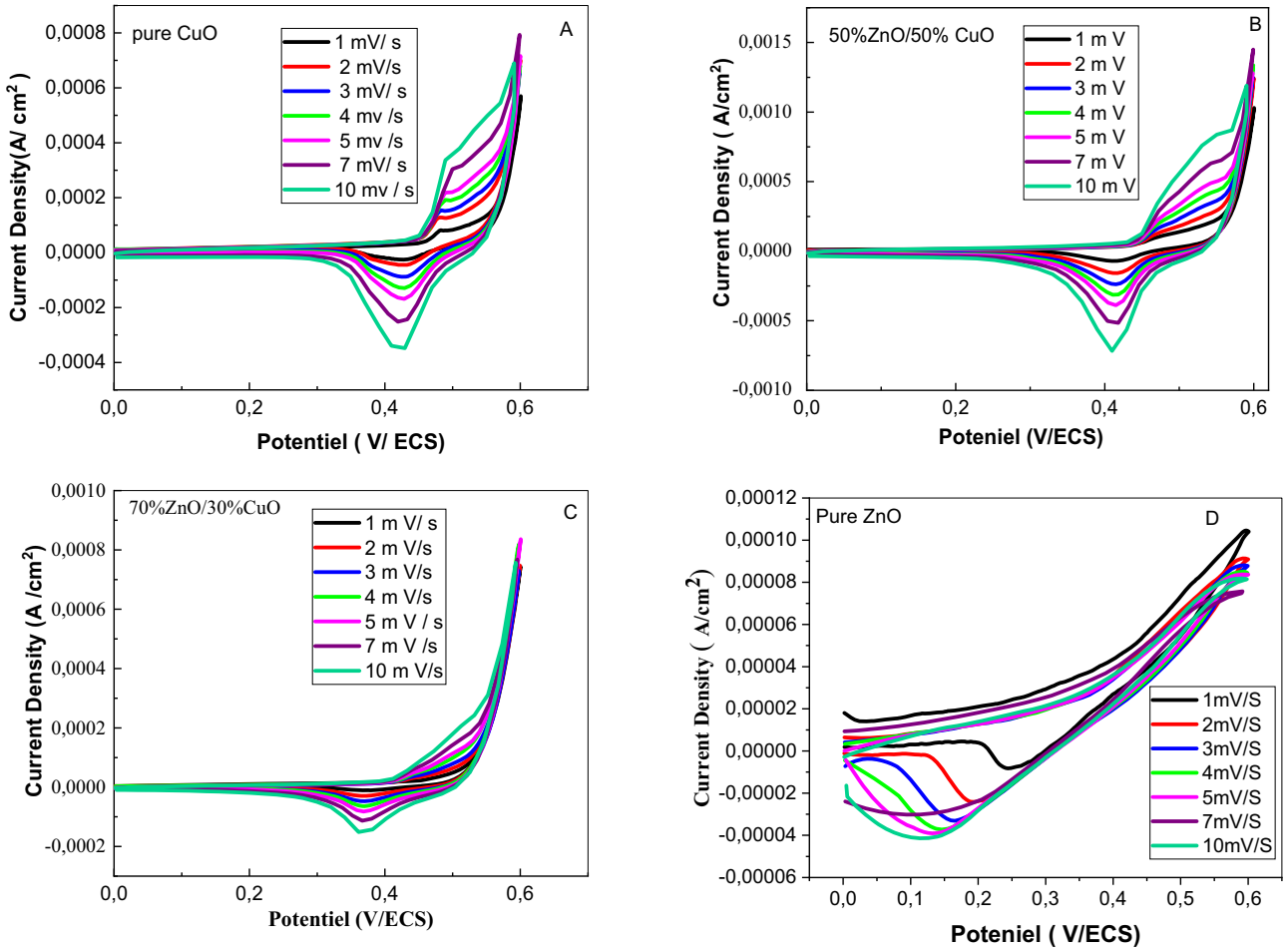

Fig. 6 Cyclic voltammograms of different electrodes (**A**–**D**) at Various scan rates for ZnO, CuO, 50%ZnO/50%CuO, and 70%ZnO/30%CuO synthetized by sol-gel route

- Cs: Specific capacitance (F/g)
- ∫I(V)dV: Integrated area of one complete cycle of CV curve
- m: Mass of the active material (m = 0.11 mg)
- ΔV : Potentiel Windows (V)
- v: Scan rate (V/S)

Figure 8 illustrates the specific capacitance decreases with increasing scan rates for all samples; the values at a scan rate of 1 mV/S were calculated to be:

Pure CuO: 98.77 F/g, Pure ZnO: 78.73 F/g, 70% ZnO/ 30% CuO: 77.73 F/g, and 50% ZnO/50% CuO: 217.81 F/g. The superior specific capacitance of the 50% ZnO – 50% CuO composition is due to its large surface area, resulting from the reduced size of its crystallites [35].

Table 4 shows that the 50% ZnO/50% CuO electrode exhibits high capacitance and excellent stability like other composite materials.

To investigate the charge storage mechanisms and electrochemical behavior of the materials, the current density was plotted as a function of the square root and logarithm of the scan rate (Fig. 9). A linear relationship log (Ip)-log (scan rate) was obtained, suggesting a charge storage process controlled mainly by diffusion. Meanwhile, plotting the current density as a function of the logarithm of the scan rate provides information on the capacitive behavior, distinguishing surface-controlled processes from diffusion-limited mechanisms [6, 36].

GCD tests were performed on 50%ZnO/50%CuO at various current densities. As shown in Fig. 10, the material exhibits battery-type behavior, confirming the involvement of faradaic reactions during the charge and discharge cycles [6, 36–40].

Figure 11 illustrates the specific capacitance retention of the 50%ZnO/50%CuO electrode after 5000 cycles. The retention, 96% of the initial capacitance, indicates the excellent electrochemical stability of this material.

The electrochemical impedance spectroscopy (EIS) analysis provides insights into the charge transfer kinetics, ion transport mechanisms, and interfacial properties of the

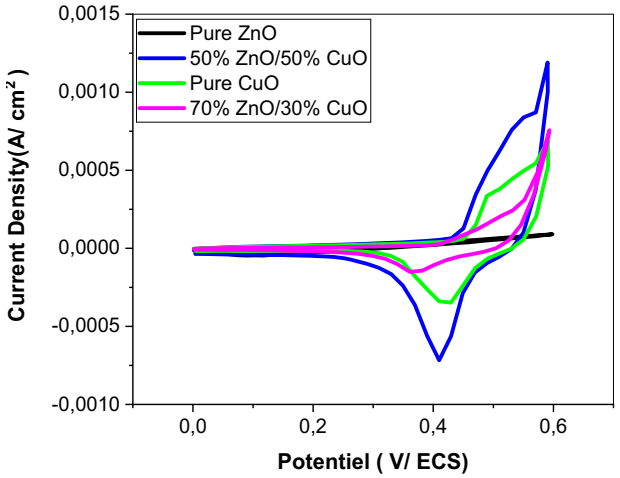

Fig. 7 Cyclic voltammograms of different samples at 10 mV/S for pure ZnO, pure CuO, 50%ZnO/50%CuO, and 70%ZnO/30%CuO synthesis by sol-gel route

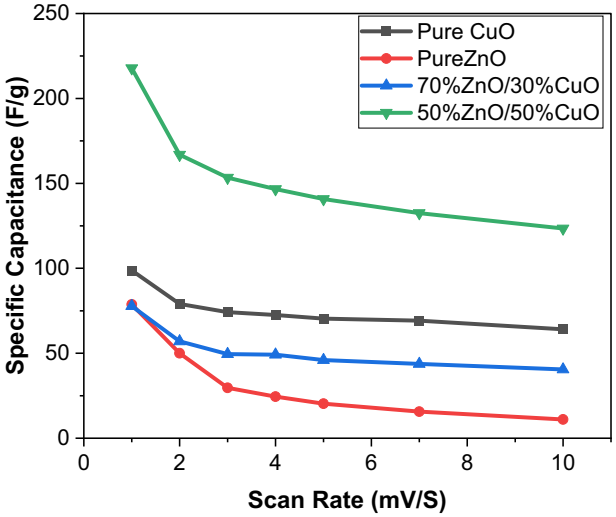

Fig. 8 Specific capacitance as a function of the scan rate determined from CV curves for ZnO, CuO, 50%ZnO/50%CuO and 70%ZnO/30% CuO

Table 4 Comparison of the specific capacitance of different electrodes

Composite material	Synthesis method	Electrolyte	Specific capacitance	Cyclic retention (%)	Refs.
ZnO Nps	Co-precipitation	3 M KOH	86.4 F/g (2 mV.s^{-1})	97% after 2000 cycles	[41]
ZnO/rGO	Chemical	2 M KOH	185.4 (15 mV.s^{-1})	Not reported	[42]
CuO/ZnO	Co-precipitation	Not Reported	208 (5 mV.s^{-1})	Not reported	[43]
ZnO/AC	One Step Electrospinning	6 M KOH	178.2 (25 mV.s^{-1})	Not reported	[44]
Graphene/ZnO	Hydrothermal	0.5 M Na_2SO_4	156 (5 mV.s^{-1})	Not reported	[45]
NiO-ZnO/graphene oxide (GO)	Co-precipitation	1 M Na_2SO_4	1690 F.g^{-1} (10 mV s^{-1})	Not reported	[46]
PVP-capped $Ni(OH)_2$/NiO	Chemical bath deposition	1 M KOH	1184 F.g^{-1} (0.5 mA.cm^{-2})	Not reported	[47]
Nanosheet-like CuO	successive ionic layer adsorption	0.5 M $NaSO_4$	566.33 F.g^{-1} (5 mV s^{-1})	100% after 1000 cycles	[48]
Gr/ZnO/$Ni(OH)_2$	Electro-deposition	4 M KOH	545.5 mF.cm^{-2} (1 mA.cm^{-2})	92.7% after 10 000 cycles	[37]
NiO/C	Template assisted hydrothermal	2 M KOH	686 F.g^{-1} (1 A.g^{-1})	100% after 5000 cycles	[38]
Ultrathin a-$Ni(OH)_2$	chemical deposition method	2 M KOH	562 F.g^{-1}	62% after 500 cycles	[39]
50%ZnO/50%CuO	Sol-gel	1 M KOH	217.81 (1 mV.s^{-1})	96% after 5000 cycles	This work

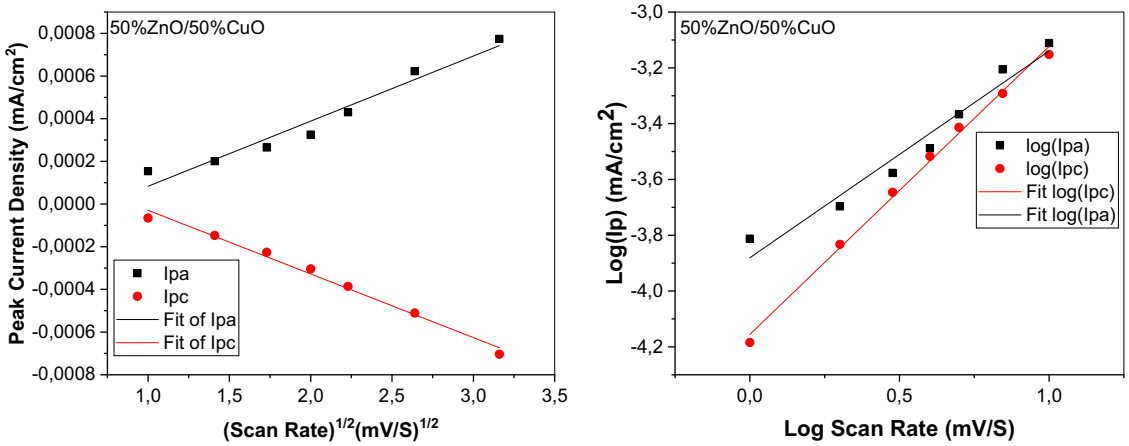

Fig. 9 Plots of peak current density vs. (scan rate)$^{1/2}$ and relationship log (Ip)-log (scan rate)

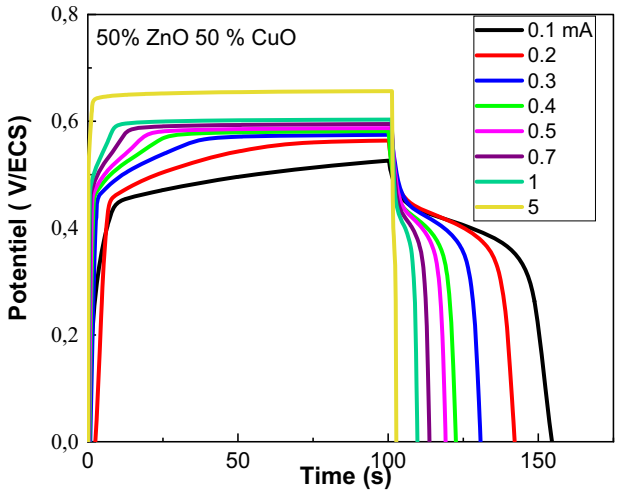

Fig. 10 GCD curve of electrode at different currents densities

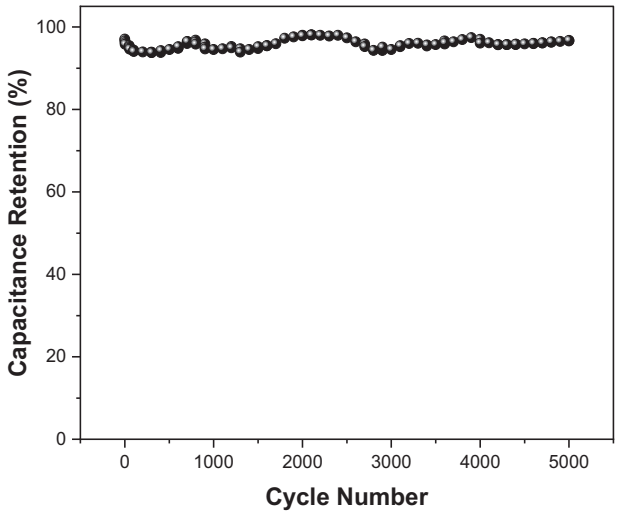

Fig. 11 Cyclic tability of 50% ZnO/50% CuO at a current density of 0.1 mA/cm^2

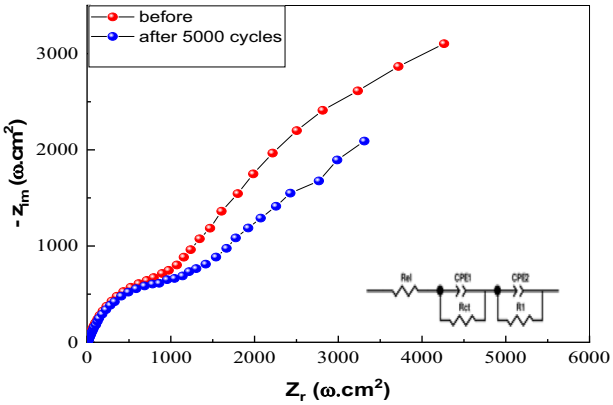

Fig. 12 EIS plots of nano-composite 50% ZnO- 50% CuO electrode before and after 5000 cycles

Table 5 Electrochemical parameters for 50% ZnO/50% CuO nano-composite

	R_{el} (Ω cm^{-2})	CPE1 (mF cm^{-2})	n_1	R_{ct} (Ω cm^{-2})	CPE2 (mF cm^{-2})	n_2	R_1 (Ωcm^{-2})
Before	4.47	0.331	0.76	737.54	2.009	0.89	6949
After 5000 cycles	5.35	0.309	0.88	950.4	1.25	0.57	7000

50% ZnO/50% CuO nanocomposite, before and after 5000 charge-discharge cycles.

The Nyquist plots (Fig. 12) illustrate the evolution of electrochemical parameters (Table 5), including electrolyte resistance (Rel), charge transfer resistance (Rct), material transfer resistance (R1), and constant phase elements (CPE1 and CPE2). These variations highlight the impact of cycling on the electrode's electrochemical behavior.

The resistance (Rel), which represents the intrinsic resistance of the electrolyte and electrode contacts, remains almost constant (4.47 to 5.35 Ω·cm^2) after 5000 cycles. This slight increase can be attributed to slight changes at the electrode/electrolyte interface or variations in the electrolyte composition during cycling. The first constant phase element (CPE1), which models the double layer capacitance and interfacial charge storage, decreases slightly, from 0.331 to 0.309 mF·cm^{-2}, while its exponent n1 increases from 0.76 to 0.88. These results suggest an improvement in the homogeneity of the charge distribution, due to the activation and restructuring of the electrode during cycling. The resistance Rct, which quantifies the difficulty of electron transfer at the electrode/electrolyte interface, increases from 737.54 to 950.4 Ω•cm² after 5000 cycles. This moderate increase suggests:

A slight degradation in charge transfer efficiency, likely due to the formation of resistive surface layers or minor electrode aging.
Reduced accessibility to electroactive sites, slightly increasing polarization effects.

The moderate increase in Rct suggests a slight decrease in charge transfer efficiency, but remains within an acceptable range for stable long-term cycling. The increase in R1 reflects minor changes in ion transport properties, but the material retains reasonable ionic conductivity. The decrease in CPE2 and the reduction in n2 indicate a change in charge storage behavior, likely reflecting changes in the pseudo-capacitive contribution. Overall, the 50% ZnO/50% CuO Nano-composite exhibits good electrochemical stability after 5000 cycles, with minimal degradation in charge

transfer and ion transport, making it a promising material for supercapacitor applications.

4 Conclusion

The simple sol-gel route was successfully used for the synthesis of ZnO, CuO and ZnO/CuO Nano-composites. The incorporation of monoclinic tenorite CuO within Wurtzite ZnO has been confirmed by X-ray diffraction. Increasing CuO concentration in ZnO/CuO Nano-composites results in a reduction in crystallite size, optical gaps and variation in surface roughness. These changes are interconnected and result from the intrinsic properties of CuO and its interaction with the ZnO matrix. These correlations are essential for optimizing the properties of ZnO/CuO Nano-composite for specific application, particularly supercapacitor. The 50% ZnO–50% CuO composite material is a promising candidate for transparent supercapacitor electrodes due to its excellent specific capacitance, efficient charge transfer, and remarkable electrochemical stability. These results provide valuable insights for the future development of advanced metal oxide materials in energy storage technologies.

Data availability

No datasets were generated or analyzed during the current study.

Acknowledgements We would like to thank Prof. Said Omeiri (University of USTHB, Algiers, Algeria) for his valuable insights concerning the interpretation of some results.

Author contributions MO Boughanem conducted the experimental part of the research in addition to writing the manuscript. N Touka supervised the work and accompanied the first author. S Mokhtari co-supervised the work, reviewed the manuscript, and provided some necessary materials. D Tabli contributed in XRD techniques. S Eddine Berrabah reviewed the English of the manuscript. S Kaizra contributed in electrochemical applications. N Selmi reviewed the manuscript. M Trari reviewed the manuscript.

Compliance with ethical standards

Conflict of interest The authors declare no competing interests.

References

1. Mahajan P, Singh A, Arya S (2020) Improved performance of solution processed organic solar cells with an additive layer of sol-gel synthesized ZnO/CuO core/shell nanoparticles. J Alloys Compd, 814, https://doi.org/10.1016/j.jallcom.2019.152292
2. Xu L, Zhou Y, Wu Z, Zheng G, He J, Zhou Y (2017) Improved photocatalytic activity of nanocrystalline ZnO by coupling with CuO. J Phys Chem Solids 106:29–36. https://doi.org/10.1016/j.jpcs.2017.03.001
3. Chen X, Huang Y, Zhang X, Li C, Chen J, Wang K (2015) Graphene supported ZnO/CuO flowers composites as anode materials for lithium ion batteries. Mater Lett 152:181–184. https://doi.org/10.1016/j.matlet.2015.03.136
4. Abed HR, Alwan AM, Yousif AA, Habubi NF (2019) Efficient SnO2/CuO/porous silicon nanocomposites structure for NH3 gas sensing by incorporating CuO nanoparticles. Opt Quantum Electron, 51, https://doi.org/10.1007/s11082-019-2046-y
5. Fatima R, Ullah N, Bilal U, Khan HA, Almutairi TM, Saleem S (2024) Facile and sustainable synthesis of metal nanoparticles (Ag, Fe, Cu, and Zn) using polyamide and polyhydrazide. J Solgel Sci Technol 111:166–176. https://doi.org/10.1007/s10971-024-06439-0
6. Wu F, Wang X, Hu S, Hao C, Gao H, Zhou S (2017) Solid-state preparation of CuO/ZnO nanocomposites for functional supercapacitor electrodes and photocatalysts with enhanced photocatalytic properties. Int J Hydrog Energy 42:30098–30108. https://doi.org/10.1016/j.ijhydene.2017.10.064
7. Bishwakarma H, Kumar Das A, Kumar P, Kumar Singh P, Awad MM (2023) Structure and electrochemical properties of CuO-ZnO nanocomposite produced by the one-step novel discharge process. J Taibah Univ Sci, 17, https://doi.org/10.1080/16583655.2023.2188017
8. Al-Khezraji AAR, Abd Ali HR, Yousif AA, Abed HR (2021) Effect of mixed ZnO/CuO nanoparticles on the structural, morphological, and topographical properties. J Phys Conf Ser, https://doi.org/10.1088/1742-6596/1963/1/012053
9. BaQais A, Alam MW, Farhan M, Muteeb G, Allag N, Mushtaq S (2023) Probe-Sonicated Synthesis of CuO–ZnO Hybrid Nanocomposite for Photocatalytic and Supercapacitor Applications. Inorganic 11:370. https://doi.org/10.3390/inorganics11090370
10. Nalbant A, Ertek Ö, Okur I (2013) Producing CuO and ZnO composite thin films using the spin coating method on microscope glasses. Mater Sci Eng B 178:368–374. https://doi.org/10.1016/j.mseb.2013.01.010
11. Mohammed EA (2022) Effect of Annealing on Sensing Properties of ZnO: CuO Nanocomposite Thin Films by the Sol-gel Method. NeuroQuantology 20:32–38. https://doi.org/10.14704/nq.2022.20.2.NQ22021
12. Nagarani S, Sasikala G, Yuvaraj M, Kumar RD, Balachandran S, Kumar M (2022) ZnO-CuO nanoparticles enameled on reduced graphene nanosheets as electrode materials for supercapacitors applications. J Energy Storage 52:104969. https://doi.org/10.1016/j.est.2022.104969
13. Bari RH, Patil SB, Bari AR (2014) Spray Pyrolised Prepared CuO–ZnO Nanocomposites Thin Films for Ethanol Sensor. Mater Focus 3:119–124. https://doi.org/10.1166/mat.2014.1143
14. Uyen VNL et al. (2020) Characteristics and antifungal activity of CuO-ZnO nanocomposites synthesised by the sol-gel technique. Vietnam J Sci Technol Eng 62:17–22. https://doi.org/10.31276/VJSTE.62(1).17-22
15. Batra N, Tomar M, Gupta V (2015) ZnO-CuO composite matrix based reagentless biosensor for detection of total cholesterol. Biosens Bioelectron 67:263–271. https://doi.org/10.1016/j.bios.2014.08.029
16. Li Y, Xu L, Li X, Shen X, Wang A (2010) Effect of aging time of ZnO sol on the structural and optical properties of ZnO thin films prepared by sol-gel method. Appl Surf Sci 256:4543–4547. https://doi.org/10.1016/j.apsusc.2010.02.044
17. Jang J, Chung S, Kang H, Subramanian V (2016) P-type CuO and Cu2O transistors derived from a sol-gel copper (II) acetate monohydrate precursor. Thin Solid Films 600:157–161. https://doi.org/10.1016/j.tsf.2016.01.036
18. Sobihana Shariffudin S, Visuvanathan NFQMF, Azahar NEA, Saad PSM, Hashim H, Mamat MH (2022) Different Composition Ratio of ZnO/CuO Nanocomposite Thin Film using Sol-gel Spin Coating Technique. J Phys Conf Ser, https://doi.org/10.1088/1742-6596/2312/1/012044

19. Kecira Z et al. (2023) Synthesis of oxygen-functionalized biomass-based activated carbon as supercapacitor with improved electrochemical performance. Appl Phys A Mater Sci Process, 129, https://doi.org/10.1007/s00339-023-07141-8
20. Taufique MFN, Haque A, Karnati P, Ghosh K (2018) ZnO–CuO Nanocomposites with Improved Photocatalytic Activity for Environmental and Energy Applications. J Electron Mater 47:6731–6745. https://doi.org/10.1007/s11664-018-6582-1
21. Abdul-Ameer Aboud N, Alkayat WMS, Hussain DH, Rheima AM (2020) A comparative study of ZnO, CuO and a binary mixture of ZnO0.5-CuO0.5with nano-dye on the efficiency of the dye-sensitized solar cell. J Phys Conf Ser. https://doi.org/10.1088/1742-6596/1664/1/012094
22. Saleem S et al. (2025) A comparative analysis of optical and electrical properties of pure CuO and Zn doped CuO nanoparticles for optoelectronic device applications. J Solgel Sci Technol 113:213–224. https://doi.org/10.1007/s10971-024-06591-7
23. Abbas N et al. (2023) Synthesis and characterization of Fe-substituting BaO nanoparticles by sol-gel method. Dig J Nanomater Biostruct 18:1327–1338. https://doi.org/10.15251/DJNB.2023.184.1327
24. Allaf RM, Hope-Weeks LJ (2014) Synthesis of ZnO-CuO nanocomposite Aerogels by the sol-gel route. J Nanomater, 2014, https://doi.org/10.1155/2014/491817
25. Mubeen K et al. (2023) Band structure tuning of ZnO/CuO composites for enhanced photocatalytic activity. J Saudi Chem Soc, 27, https://doi.org/10.1016/j.jscs.2023.101639
26. Saleem S et al. (2024) A band gap engineering for the modification in electrical properties of Fe3O4 by Cu2+ doping for electronic and optoelectronic devices applications. J Solgel Sci Technol 109:471–482. https://doi.org/10.1007/s10971-023-06287-4
27. Cao L, Kiely J, Piano M, Luxton R (2019) A copper oxide/zinc oxide composite nano-surface for use in a biosensor. Materials, 12, https://doi.org/10.3390/ma12071126
28. Saravanakkumar D et al. (2018) Synthesis and characterization of ZnO–CuO nanocomposites powder by modified perfume spray pyrolysis method and its antimicrobial investigation. J Semiconductors 39:033001
29. Li B, Wang Y (2010) Facile synthesis and photocatalytic activity of ZnO-CuO nanocomposite. Superlattices Microstruct 47:615–623. https://doi.org/10.1016/j.spmi.2010.02.005
30. Saravanan R, Karthikeyan S, Gupta VK, Sekaran G, Narayanan V, Stephen A (2013) Enhanced photocatalytic activity of ZnO/CuO nanocomposite for the degradation of textile dye on visible light illumination. Mater Sci Eng C 33:91–98. https://doi.org/10.1016/j.msec.2012.08.011
31. Widiarti N, Sae JK, Wahyuni S (2017) Synthesis CuO-ZnO nanocomposite and its application as an antibacterial agent. In IOP Conference Series: Materials Science and Engineering, Institute of Physics Publishing, 2017. https://doi.org/10.1088/1757-899X/172/1/012036
32. Chinnaiah K et al. (2024) Enhancing supercapacitor and antimicrobial performance of bioengineered Ag/Mn3O4 composite nanorods. J Ind Eng Chem, https://doi.org/10.1016/j.jiec.2024.12.023
33. Chinnaiah K, Kannan K, Krishnamoorthi R, Palko N, Gurushankar K (2024) Nanostructured Ag/NiO composites for supercapacitor and antibacterial applications, and in-silico theoretical investigation. Journal of Physics and Chemistry of Solids, 184, https://doi.org/10.1016/j.jpcs.2023.111730
34. Wang G, Zhang L, Zhang J (2012) A review of electrode materials for electrochemical supercapacitors. Chem Soc Rev 41:797–828. https://doi.org/10.1039/c1cs15060j
35. Sivakumar S, Robinson Y, Mala NA (2022) Studies on photocatalytic performance and supercapacitor applications of undoped and Cu-doped ZnO nanoparticles. Appl Surface Sci Adv, 12, https://doi.org/10.1016/j.apsadv.2022.100344
36. Zhang L, Zhao XS (2009) Carbon-based materials as supercapacitor electrodes. Chem Soc Rev 38:2520–2531. https://doi.org/10.1039/b813846j
37. Berrabah SE, Benchettara A, Smaili F, Benchettara A, Mahieddine A (2023) High performance hybrid supercapacitor based on electrochemical deposed of nickel hydroxide on zinc oxide supported by graphite electrode. J Alloy Compd 942:169112. https://doi.org/10.1016/j.jallcom.2023.169112
38. Chime UK et al. (2020) Recent progress in nickel oxide-based electrodes for high-performance supercapacitors. Curr Opin Electrochem 21:175–181. https://doi.org/10.1016/j.coelec.2020.02.004
39. Obodo RM et al. (2020) Recent advances in metal oxide/hydroxide on three-dimensional nickel foam substrate for high performance pseudocapacitive electrodes. Curr Opin Electrochem 21:242–249. https://doi.org/10.1016/j.coelec.2020.02.022
40. Wang G, Huang J, Chen S, Gao Y, Cao D (2011) Preparation and supercapacitance of CuO nanosheet arrays grown on nickel foam. J Power Sources 196:5756–5760. https://doi.org/10.1016/j.jpowsour.2011.02.049
41. Shaheen I, Ahmad KS, Zequine C, Gupta RK, Thomas AG, Azad Malik M (2022) Sustainable synthesis of organic framework-derived ZnO nanoparticles for fabrication of supercapacitor electrode. Environ Technol 43:605–616. https://doi.org/10.1080/09593330.2020.1797899
42. Rattanaveeranon S, Jiamwattanapong K (2022) Effect of CuO/rGO and ZnO/rGO Hybrid Additional Layers on Supercapacitor Performance. Trends Sci 19, https://doi.org/10.48048/tis.2022.5603.
43. Suganthi N, Thangavel S, Pushpanathan K (2020) Infra-Red Emission and Electrochemical Properties of CuO/ZnO Nanocubes. J Inorg Organomet Polym Mater 30:5224–5233. https://doi.org/10.1007/s10904-020-01700-9
44. Kim CH, Kim BH (2015) Zinc oxide/activated carbon nanofiber composites for high-performance supercapacitor electrodes. J Power Sources 274:512–520. https://doi.org/10.1016/j.jpowsour.2014.10.126
45. Li Z, Zhou Z, Yun G, Shi K, Lv X, Yang B (2013) High-performance solid-state supercapacitors based on graphene-ZnO hybrid nanocomposites. Available: http://www.nanoscalereslett.com/content/8/1/473
46. Obodo RM et al. (2020) Conjugated NiO-ZnO/GO nanocomposite powder for applications in supercapacitor electrodes material. Int J Energy Res 44:3192–3202. https://doi.org/10.1002/er.5091
47. Nwanya AC et al. (2015) Electrochromic and electrochemical supercapacitive properties of Room Temperature PVP capped Ni(OH)2/NiO Thin Films. Electrochim Acta 171:128–141. https://doi.org/10.1016/j.electacta.2015.05.005
48. Nwanya AC et al. (2016) Facile Synthesis of Nanosheet-like CuO Film and its Potential Application as a High-Performance Pseudocapacitor Electrode. Electrochim Acta 198:220–230. https://doi.org/10.1016/j.electacta.2016.03.064